Catalysis Today 151 (2010) 266–270

Contents lists available at ScienceDirect

Catalysis Today

journal homepage: www.elsevier.com/locate/cattod

The different impacts of SO_2 and SO_3 on Cu/zeolite SCR catalysts

Yisun Cheng [a,*], Christine Lambert [a], Do Heui Kim [b], Ja Hun Kwak [b], Sung June Cho [c], Charles H.F. Peden [b]

[a] Ford Innovation Center, Ford Motor Company, 2101 Village Road, Dearborn, MI 48124, USA
[b] Institute for Interfacial Catalysis, Pacific Northwest National Lab, Richland, WA 99352, USA
[c] Department of Applied Chemical Engineering and Center for Functional Nano Fine Chemicals (BK21 Program), Chonnam National University, Gwangju 500-757, South Korea

ARTICLE INFO

Article history:
Available online 19 February 2010

Keywords:
Urea SCR catalysts
Cu/zeolite
SO_2 and SO_3 poisoning
NOx emission control
Durability
Deactivation

ABSTRACT

The different impacts of SO_2 and SO_3 on Cu/zeolite SCR catalysts were investigated by SCR performance tests and multiple characterization techniques including temperature programmed desorption (TPD), X-ray photoelectron spectroscopy (XPS) and X-ray absorption fine structure (XAFS). The results indicate that a larger amount of highly dispersed $CuSO_4$ formed in the zeolite catalysts (Z–$CuSO_4$) upon SO_3 poisoning, explaining the much more significant deactivation of the Cu/zeolite catalysts that were exposed to SO_3 compared to poisoning by SO_2. This paper provides the first demonstration that active sites of Cu/zeolite SCR catalysts involved in the storage and removal of sulfur can react with SO_2 and SO_3 in very different ways. In particular, the significant differences in the extent of sulfur uptake account for the considerably different impacts of SO_2 and SO_3 poisoning on the performance of Cu/zeolite SCR catalysts.

1. Introduction

Cu/zeolite catalysts for the selective catalytic reduction (SCR) of NOx with aqueous urea have high de-NOx activity and superior thermal durability. As such, these catalysts are among the leading candidates for the treatment of NOx emissions for diesel vehicles required to meet Federal Tier 2 and California LEVII emission standards [1–4]. It is known that Cu/zeolite SCR catalysts are especially sensitive to sulfur poisoning [5–10]. The SCR performance of sulfur poisoned Cu/zeolite catalysts is reduced to a significant extent, although the catalysts can be regenerated by decomposing the sulfates (deSOx) at high temperatures under lean conditions. Sulfur poisoning directly impacts the overall SCR performance and durability of Cu/zeolite SCR catalysts [4–6]. This problem will remain as long as sulfur is present in the fuels and engine oils, even at the "ultra low" sulfur levels (containing less than 15 ppm sulfur) applied in the future.

Most studies on sulfur poisoning of transition metal/zeolite SCR catalysts have used SO_2 as the poisoning agent [7–10]. Insofar as diesel oxidation catalysts (DOCs) will be employed upstream of the SCR catalysts for most applications, it is likely that at least a portion of the SO_2 will be oxidized into SO_3. Our recent studies [5] showed that the NOx activity of Cu/zeolites is significantly reduced for samples poisoned by SO_3 vs. those poisoned by SO_2. The results indicated that sulfur poisoning by SO_2 and SO_3 are not equivalent, with different poisoning mechanisms and impacts. Thus, this study points to an important sulfur poisoning concern for systems with DOCs in front of SCR catalysts in diesel engine applications. To understand the different impacts of SO_2 and SO_3 on Cu/zeolite SCR catalysts, lab aged Cu/zeolite SCR catalysts were assessed by performance tests in simulated diesel exhaust gas in a lab flow reactor. The focus of this paper is to investigate and understand correlations between activity deterioration of Cu/zeolite SCR catalysts and the changes of Cu active sites after being poisoned by SO_2 and SO_3. The poisoned and regenerated (deSOxed) catalysts were characterized by X-ray photoelectron spectroscopy (XPS), temperature programmed desorption (TPD), and X-ray absorption fine structure (Cu K-edge XAFS) to develop an understanding of sulfur poisoning. The results of this study provide, for the first time, insight into the different poisoning mechanisms between SO_2 and SO_3, and also provide valuable information on the durability of SCR catalysts for lean-burn vehicle applications.

2. Experimental

The Cu/zeolite SCR catalysts used in this study were: CatA which was a fully formulated cordierite monolith with Cu/zeolite washcoat from a catalyst supplier, and CatB, a beta zeolite-based Cu/zeolite SCR catalyst that we synthesized. The CatB catalyst was prepared by ion exchange of a NH^{4+}–BEA zeolite with $Si/Al_2 = 25$, obtained from Zeolyst International (CP814E), using aqueous $Cu(NO_3)_2$ solutions. These solutions contained total Cu^{2+} ion concentrations ~250% of the zeolite cation sites. Following the ion exchange, the samples were thoroughly washed with distilled water and then dried at 120 °C in air. Ion-exchange processes were repeated 2 times to ensure 100% exchange levels. The dried CatB

---

* Corresponding author.
E-mail address: ycheng1@ford.com (Y. Cheng).

0920-5861/$ – see front matter © 2010 Elsevier B.V. All rights reserved.
doi:10.1016/j.cattod.2010.01.013

was activated at 500 °C for 2 h under flowing zero air before any catalyst characterization or performance measurement. For proprietary reasons, details of CatA cannot be given in this paper. While the type of zeolite and Cu loading in CatA may well be different than CatB, both catalysts were designed for transient diesel engine applications, and the test results showed that they both had similar deactivation behavior with respect to SO_2 and SO_3 aging. Moreover, characterization (e.g., XPS) of both catalysts studied here showed similar results after poisoning with SO_2 and SO_3, corroborating the conclusions made here.

The CatA monolith samples were cored to sizes of 1 in. diameter by 1 in. long and were aged and tested using a laboratory flow reactor at a space velocity of 30,000 h^{-1}. Before any sulfur poisoning, the samples were hydrothermally aged with 14% O_2, 5% CO_2, 4.5% H_2O, and N_2 balance, at 670 °C for 20 h. Then, the samples were exposed to 40 ppm SO_2 or SO_3 in a gas mixture containing 14% O_2, 5% CO_2, 4.5% H_2O, and N_2 balance at 200, 300, and 400 °C for 1.5 h. The total sulfur exposures corresponded to 500 sulfur-equivalent miles with 350 ppm sulfur fuel, a relatively high sulfur fuel currently available in the US.

To remove sulfur (deSOx), the sulfated samples were first heated and stabilized in the reactor at 170 °C in 14% O_2, 5% CO_2, and 4.5% H_2O and N_2 balance. Then, the stored sulfur was removed by heating the catalysts in the same gas mixture from 170 to 770 °C at a rate of 5 °C/min. The NOx performance was measured before the sulfur poisoning (Test1), after the sulfur poisoning (Test2), and after the deSOx (Test3). Steady state NOx activities of samples were measured from 130 to 340 °C in a flow reactor connected to an FTIR instrument from MIDAC Corporation with a heated sample cell for gas analysis. The SCR evaluation was stopped at 340 °C to prevent decomposition of any sulfates on the catalyst surface that were generated during the sulfur aging. For the steady state SCR activity measurements, simulated diesel exhaust gas (composition shown in Table 1) was flowed through the sample core.

Selected SO_2 and SO_3 poisoned CatA and CatB samples were characterized by XPS and Cu K-edge XAFS. XPS experiments were carried out for samples aged at 200 °C with SO_2 and SO_3. For 27 mm (1 in.) long CatA monolith core samples, 5 points, separated by a distance of 6 mm, were analyzed in the analysis chamber of a Physical Electronics Instruments Quantum 2000 using Al Kα X-rays and a pass energy of 71 eV. The position and intensity of the Al 2s peak at 119.2 eV were used as references. CatB samples were analyzed with XPS in the powder form, after the treatment with SO_2 or SO_3.

Cu K-edge XAFS measurements were carried out for CatB samples at beam line X19A of the National Synchrotron Light Source (NSLS) at Brookhaven National Laboratory. The X19A beamline used to collect the Cu K-edge XANES data is equipped with a double-crystal Si(1 1 1) monochromator. Fluorescence measurements were performed using a passivated implanted planar silicon (PIPS) detector (Canberra Industries, CT). The beam path from the incident ion chamber to the sample chamber was purged with He gas. A small amount of well-mixed sample was evenly spread over double-sided tape. The X-ray energy for the K-edge of Cu metal was used for calibrating the energy scale. The statistical noise at X19A is better than 0.001%. Structural parameters were obtained through curve fitting using Athena and Artemis programs packaged in the theoretical Feff8 computer code, IFEFFIT 8.0.

Table 1
Composition of the simulated diesel exhaust gas mixture used for SCR activity measurements.

Component	O_2	H_2O	CO_2	NO	NH_3	N_2
Concentration	14%	4.5%	5%	350 ppm	350 ppm	Balance

3. Results and discussion

3.1. The impacts of SO_2 and SO_3 poisoning on Cu/zeolite SCR catalyst activity

Previous studies [6] have shown that the impact of sulfur was mainly on the low temperature NOx activity for Cu-based zeolite SCR catalysts, and that stored sulfur starts to release from the catalyst around 350 °C under lean deSOx conditions. As such, the measurements of NOx performance of sulfur-aged SCR catalysts were limited to temperatures below 340 °C in this study. The NOx activities for CatA samples before and after sulfur poisoning by SO_2 at 200, 300, and 400 °C are shown in Fig. 1. The NOx activity of Cu/zeolite SCR catalysts decreased to a relatively small extent after being exposed to 40 ppm SO_2 for 1.5 h regardless of the SO_2 aging temperatures. The lower SO_2 aging temperature resulted in higher NOx activity decreases: the NOx activities performed at 178 °C decreased by 33%; by 21% for the sample aged at 300 °C, and only by 8% for the sample aged at 400 °C. Fig. 2 shows the NOx activity of CatA Cu/zeolite catalysts before and after sulfur poisoning by SO_3 at 200, 300, and 400 °C. The NOx activities were significantly decreased for all samples after being exposed to 40 ppm SO_3 for 1.5 h regardless of the exposure temperatures, with NOx activities of all samples being extremely low at $T < 250$ °C. The sample aged with SO_3 at lower temperature had better NOx activity between 250 and 340 °C. Notably at a 340 °C test temperature, the NOx activity of the sample aged at 200 °C was close to 100%, while the NOx activity of sample aged at 400 °C showed only 70% conversion.

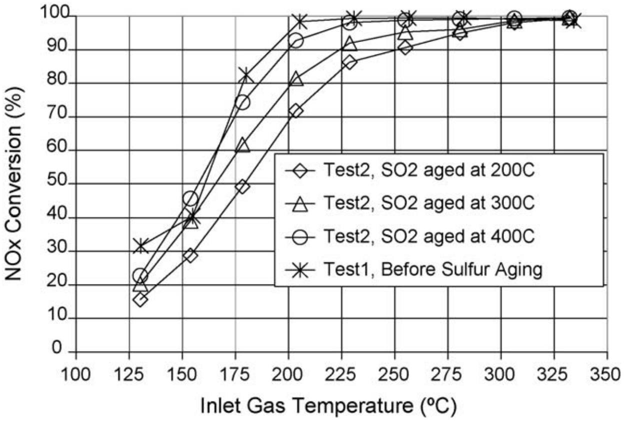

Fig. 1. Steady state NOx conversions for CatA Cu/zeolite SCR catalysts before and after SO_2 aging at 200, 300, and 400 °C.

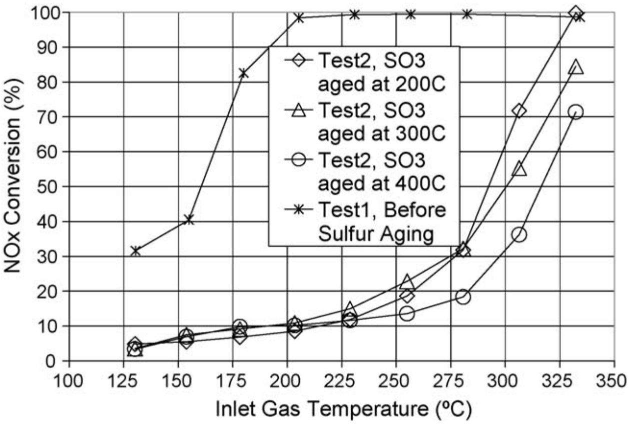

Fig. 2. Steady state NOx conversions for CatA Cu/zeolite SCR catalysts before and after SO_3 aging at 200, 300, and 400 °C.

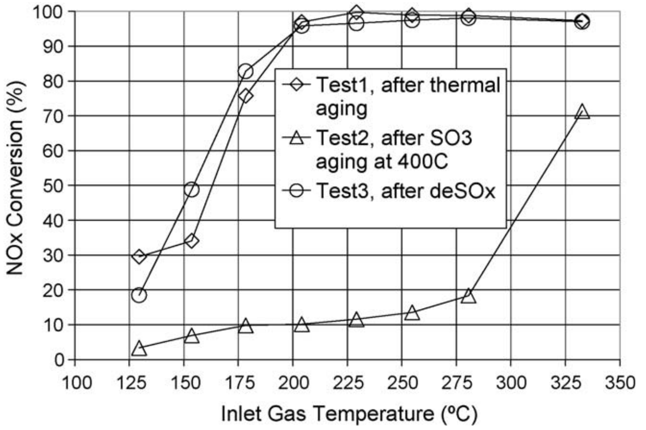

Fig. 3. Steady state NOx conversions for CatA Cu/zeolite SCR catalysts before and after SO_3 aging at 400 °C, and after the deSOx.

Fortunately, NOx activity was restored for all sulfur-aged samples after carrying out a deSOx process, even for catalysts that were significantly deactivated by the SO_3 aging. As an example, Fig. 3 shows the NOx activity of SO_3 aged CatA Cu/zeolite before the sulfur poisoning (Test1), after the sulfur poisoning by SO_3 at 400 °C (Test2), and after the deSOx (Test3). This figure demonstrates that the NOx activities in Test3 were essentially the same as those in Test1, indicating that CatA regained full SCR function after the deSOx. SO_2 was the main sulfur compound released during the deSOx for the samples aged with SO_2 or SO_3. During the deSOx procedure, the amounts of SO_2 released from the SO_3 aged CatA Cu/zeolite SCR catalysts were 5–15 times higher than those from the SO_2 aged samples as shown in Fig. 4. Since the released SO_2 depends on the surface coverage, these results suggest that the samples aged with SO_3 had much higher sulfur coverages compared to those aged with SO_2. In other words, comparing to SO_2, SO_3 tended to remain/store more on the CatA Cu/zeolite SCR catalysts even though the total sulfur(S) exposures were same for all the samples poisoned by SO_2 and SO_3. (Note that, although the total sulfur(S) exposures were the same for all the samples poisoned by SO_2 and SO_3 before the deSOx, no sulfur measurement was made during this process. As such, we are not able to estimate sulfur coverages before the deSOx.) The results so far indicate that the active sites of Cu/zeolite SCR catalysts involved in sulfur storage and removal react with SO_2 and SO_3 in very different ways.

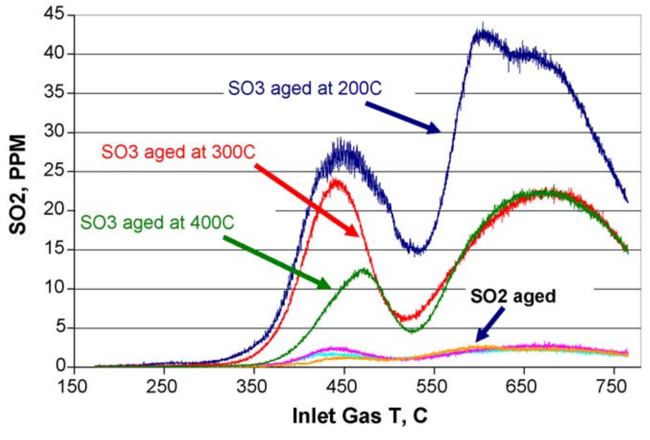

Fig. 4. Released SO_2 from CatA Cu/zeolite SCR catalysts aged with SO_2 or SO_3 observed during the deSOx process.

3.2. The characterizations of SO_2 and SO_3 poisoned Cu/zeolite SCR catalysts

There is little available literature to explain SO_3 poisoning mechanisms of Cu/zeolite SCR catalysts. Ramachandran et al. [7] observed that V–ZSM-5 catalysts exhibit stable activity for NO reduction in the presence of H_2O and SO_2 but rapidly deactivate in the presence of 10 ppm SO_3. These authors attributed the possible SO_3 deactivation to the formation of ammonium (bi)sulfate when both NH_3 and SO_3 are present. However, there was no NH_3 during the aging in this study and, therefore, it is not likely that ammonium (bi)sulfate formation can explain the results presented here.

In order to obtain the information on the oxidation state and amount of sulfur species, we applied X-ray photoelectron spectroscopy (XPS) for the CatA samples treated at 200 °C with SO_2 and SO_3. For the 27 mm (1 in.) long monolith samples, 5 points were analyzed separated by a distance of 6 mm, allowing us to determine the spatial distribution along the monolith *z*-axis. Spectra of both samples contain a single peak at 169 eV, indicating that only sulfates (SO_4^{2-}) are formed by the interaction with either SO_2 or SO_3. However, there was a drastic difference in the amount of sulfate species between the samples treated with SO_2 or SO_3. As shown in Fig. 5, the sample treated with SO_3 clearly had larger amounts of sulfur, especially up to 13 mm from the inlet, followed by a significant decrease thereafter. We suggest that sulfate saturates the catalyst from the inlet, gradually moving toward the outlet. In contrast, the sample treated with SO_2 had considerably smaller amount of sulfur in the inlet and along the monolith. The summed amounts of sulfur along the monolith indicates that the sample treated with SO_3 contained at least 5 times larger concentrations than the one treated with SO_2, which points to the relative ease of sulfate formation by reaction with SO_3. XPS results on the samples after the desulfation (deSOx) showed essentially no sulfur remained on the surface of the catalyst (not shown). This result implies that all sulfates are desorbed as a result of thermal desorption during the deSOx, as evidenced also by the larger desorption of SO_2 during the deSOx for the sample treated with SO_3 than one treated with SO_2, and the full recovery of the activity as shown in Fig. 3.

In addition to CatA samples, we also performed similar XPS analyses of the CatB samples. As shown in Fig. 6, the samples

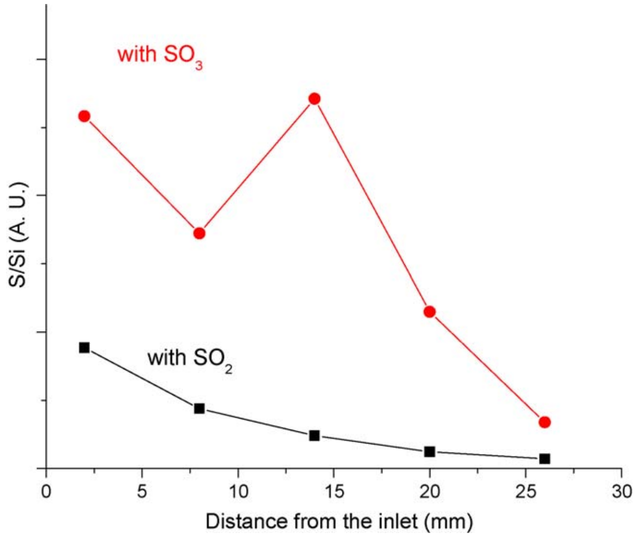

Fig. 5. Distribution of sulfur, plotted as normalized S/Si ratios, as a function of distance from the inlet of the monolith-type CatA sample.

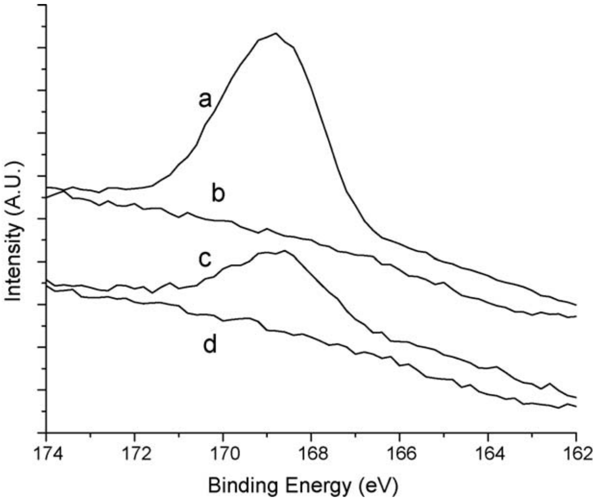

Fig. 6. S 2p XPS spectra for various CatB samples: (a) following SO_3 treatment at 200 °C and (b) after DeSOx; and (c) following SO_3 treatment at 300 °C and (d) after deSOx.

sulfated with SO_3 contained measurable amounts of sulfate on the surface, while the one sulfated with SO_2 (spectrum not shown) did not have any observable sulfur species. Note that the sample sulfated with SO_3 at 200 °C has a larger peak of sulfate than the sulfated sample prepared at 300 °C, thus accounting for the relative SO_2 desorption amounts observed during deSOx of CatA samples as shown in Fig. 4. After the deSOx, both samples contained no XPS-observable sulfur species on the surface, again suggesting that the high temperature treatment resulted in complete removal of adsorbed sulfur as SO_2 gas, consistent with the XPS results for CatA.

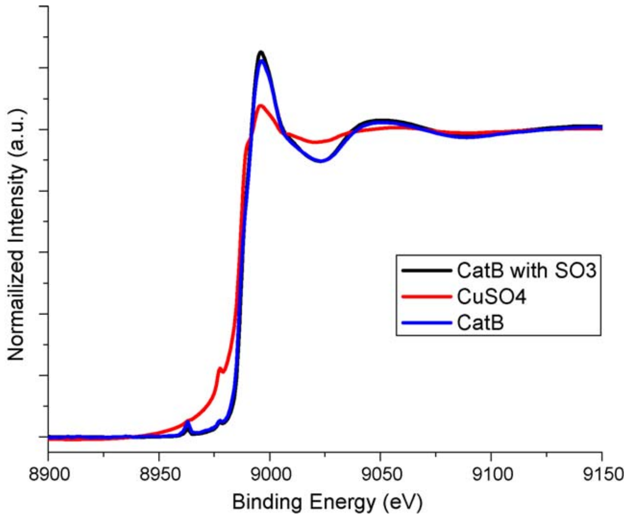

Fig. 7. Cu XANES spectra of $CuSO_4$, freshly aged CatB (unsulfated) and SO_3 treated CatB.

Table 2
Summary of XAFS curve fitting for Cu in the CatB sample using Feff7 and FEFFIT[a].

Sample	Pair	CN[b]	r (nm)[c]	a^2 (pm^2)[d]	AE (eV)
Cu aged	Cu–O	3.5 ± 0.5	0.195 ± 0.001	57 ± 11	−3.4 ± 2.1
CuZ desulfated	Cu–O	3.4 ± 0.3	0.195 ± 0.001	54 ± 8	−3.4 ± 1.4
CuZ sulfated	Cu–O	3.5 ± 0.3	0.195 ± 0.001	46 ± 6	−3.5 ± 1.2

[a] The many body reduction factor was fixed to 0.9. The fitting ranges were 20–139 nm^{-1} for Δk and 0.100–0.300 nm for Δr, respectively. The restraint was applied to the Debye–Waller factor for the multiple scattering.

[b] Coordination number.

[c] Coordination distance.

[d] The Debye–Waller factor accounting thermal and statistical vibration.

Finally, we used XANES/EXAFS analyses to investigate properties of the copper species before and after sulfation with SO_3. Fig. 7 shows the Cu K-edge XANES spectra for the CatB samples before and after SO_3 sulfation, as well as the spectra for $CuSO_4$ as a reference. The XANES spectra between 8975 and 8985 eV were similar for both unsulfated and SO_3 sulfated samples, but quite different from the spectrum of bulk $CuSO_4$. This suggests that the sulfate formation resulting from SO_3 treatment does not induce any macroscopic changes in the Cu species; in other words, Cu remains in a highly dispersed state as its initial ion-exchange locations. This behavior also is similar to that observed by Hamada et al. [11] for a Cu–ZSM-5 catalyst after SO_2/O_2 treatment.

The EXAFS region of the data shown in Fig. 7 was analyzed to get more specific information about the coordination of Cu after SO_3 sulfation and freshly aged (unsulfated). Table 2 summarizes the EXAFS curve fitting for these samples. The freshly aged CatB sample contains Cu–O bonds with a coordination number of 3.5 and bond distance of 0.195 nm, consistent with previous EXAFS analyses of a fresh Cu–BEA sample [12]. After treatment with SO_3, CatB maintains similar Cu–O bond coordination, indicating that sulfate species bound to Cu do not induce changes in the local structure of Cu within the zeolite framework. Similarly, subsequent desulfation does not change the Cu–O coordination or bond distance in the CatB catalyst. It is noteworthy that significant Cu–Cu coordination was not observed even after desulfation, suggesting that the copper species in the samples has not sintered. Taken together, these results explain the reversible recovery of activity after a deSOx process at elevated temperatures.

The above results are consistent with a previous report by Hass and Schneider [13] that used density functional calculations to show that Z–$CuSO_4$ are the energetically most stable adsorbed SOx species compared to Z–$CuSO_3$ or Z–$CuSO_2$. Upon sulfation with SO_3, sulfur exists in a highly dispersed Z–$CuSO_4$ form (as distinguished from bulk $CuSO_4$). Furthermore, the lowered affinity of the Cu–zeolite catalysts for SO_2 can be rationalized by these prior calculations.

4. Conclusions

The NOx activity results described here show that SO_3 poisoning causes much more significant deactivation of Cu/zeolite catalysts than SO_2. XPS data indicate that the sample sulfated with SO_3 contains markedly larger amounts of sulfur, present as sulfates (SO_4^{2-}) with an XPS peak at 169 eV, than the one sulfated with SO_2. XANES/EXAFS analyses further demonstrate that sulfate formation does not induce measurable changes in the state of Cu; in other words, Cu remains in a highly dispersed state at zeolite ion-exchange sites as before sulfation with SO_3. In particular, the EXAFS analyses confirm that sulfate formation as a result of SO_3 exposures does not induce changes in the local structure of Cu within the zeolite structure. Thus, we propose that sulfur exists as highly dispersed $CuSO_4$ in the zeolite (Z–$CuSO_4$). The calculated lower stability of Z–$CuSO_3$ and Z–$CuSO_2$ species [13] may explain the much lower observed levels of sulfate formed following exposures to SO_2 described here. This then explains why SO_3 poisoning causes much more significant deactivation for the Cu/zeolite catalysts than SO_2 poisoning. The results of this paper provide the first direct characterization of differences in the poisoning mechanisms between SO_2 and SO_3, and also provide valuable information for the maintenance of Cu/zeolite SCR catalyst performance for diesel vehicle applications.

Acknowledgements

Financial support for studies performed at Pacific Northwest National Laboratory (PNNL) was provided by the U.S. Department of Energy (DOE), Office of Energy Efficiency and Renewable Energy, Vehicle Technologies Program. Portions of the work were performed in the Environmental Molecular Sciences Laboratory (EMSL) at PNNL. The EMSL is a national scientific user facility supported by the U.S. DOE's Office of Science, Biological and Environmental Research. PNNL is a multi-program national laboratory operated for the U.S. Department of Energy by Battelle Memorial Institute under Contract DE-AC06-76RLO 1830. Use of the National Synchrotron Light Source at Brookhaven National Laboratory, was supported by the U.S. DOE's Office of Science, Basic Energy Sciences, under Contract No. DE-AC02-98CH10886.

References

[1] C. Lambert, J. Vanderslice, R. Hammerle, R. Belaire, Application of Urea SCR to Light-Duty Diesel Vehicles, SAE 2001-01-3623.
[2] C. Lambert, R. Hammerle, R, McGill, M. Khair, C. Sharp, Technical Advantages of Urea SCR for Light-Duty and Heavy-Duty Diesel Vehicle Applications, SAE 2004-01-1292.
[3] S.J. Schmieg, J.-H. Lee, Evaluation of Supplier Catalyst Formulations for the Selective Catalytic Reduction of NOx with Ammonia, SAE 2005-01-3881.
[4] G. Cavataio, J. Girard, J. Patterson, C. Montreuil, Y. Cheng, C. Lambert, Laboratory Testing of Urea-SCR Formulations to Meet Tier 2 Bin 5 Emissions, SAE 2007-01-1575.
[5] Y. Cheng, C. Montreuil, G. Cavataio, C. Lambert, The Effects of SO_2 and SO_3 Poisoning on Cu/Zeolite SCR Catalysts, SAE 2009-01-0898.
[6] Y. Cheng, C. Montreuil, G. Cavataio, C. Lambert, Sulfur Tolerance and DeSOx Studies on Diesel SCR Catalysts, SAE 2008-01-1023.
[7] B. Ramachandran, R.G. Herman, S. Choi, H.G. Stenger, C.E. Lyman, J.W. Sale, Catal. Today 55 (2000) 281.
[8] M. Shibata, H. Nagata, S. Takeshima, K. Hoshino, A Study of Engine Oil Composition Effects on Zeolite-type SCR Catalyst Durability, SAE 2007-01-1924.
[9] I.S. Nam, S.T. Choo, D.J. Koh, Y.G. Kim, Catal. Today 38 (1997) 181.
[10] A. Palomares, J. Prato, A. Corma, Catal. Today 75 (2002) 367–371.
[11] H. Hamada, N. Matsubayashi, H. Shimada, Y. Kintaichi, T. Ito, A. Nishijima, Catal. Lett. 5 (1990) 189.
[12] S. Dzwigaj, J. Janas, J. Gurgul, R.P. Socha, T. Shishido, M. Che, Appl. Catal. B 85 (2009) 131.
[13] K.C. Hass, W.F. Schneider, Phys. Chem. Chem. Phys. 1 (1999) 639.